FEM Modeling of Surface Losses in Accordance with Their Nature

FEM Modeling of Surface Losses in Accordance with Their Nature

Zbigniew Gmyrek
Institute of Mechatronics & Information Systems
Lodz University of Technology
Lodz, Poland
zbigniew.gmyrek@p.lodz.pl

Silvio Vaschetto, Senior *Member, IEEE*
Politecnico di Torino
Dipartimento Energia
Torino, Italy
silvio.vaschetto@polito.it

Andrea Cavagnino, *Fellow, IEEE*
Politecnico di Torino
Dipartimento Energia
Torino, Italy
andrea.cavagnino@polito.it

***Abstract*— The paper presents a new method to estimate the surface losses caused by the non-sinusoidal spatial distribution of the magnetic field, moving over the surface of laminated rotor cores. The rotating magnetic field present in the air gap of ac electrical machines causes additional losses, which are very important during motor design, in particular for high-speed applications. A simplified - but still consistent in its nature - finite element method model has been developed to simulate the mechanism of the surface loss generation. The obtained results are critically discussed and compared with those reported in other research works.**

Keywords— ac electrical machines, induction motors, rotating magnetic field, slotting effect, surface losses, additional losses, FEM modeling.

I. INTRODUCTION

The positioning of the electrical machine windings into discrete slots, as well as the presence of slot openings on the stator and rotor cores, introduce high order space harmonics in the spatial distribution of the air gap magnetic induction. The resulting non-sinusoidal magnetic field at the machine air gap generates additional Joule losses on the rotor surface. The phenomenon has been analyzed for years, and the literature reports several studies related to the winding distribution on the generation of space harmonics, as well as proposals for special winding layouts to limit these additional rotor losses [1], [2]. In detail, higher space harmonics have a relatively small amplitude compared to the fundamental harmonic of the magnetic field existing in the air gap. However, they move with respect to the rotor at much faster speeds than the fundamental harmonic. Therefore, the eddy current losses that appear on the rotor surface should be accurately modeled, especially in the era of energy-saving motors production, where the aim is to achieve the highest possible efficiency.

Recent research works concerning this type of surface losses focus on two main cases: (i) relatively large-sized solid elements (e.g. permanent magnets), and (ii) thin-laminated ferromagnetic cores (e.g. 0.5 mm stacked magnetic sheets). In both the cases, additional Joule loss occurs in the area close to the surface adjacent to the air gap, where higher space harmonics exist. The phenomenon results particularly severe for permanent magnet machines because the eddy currents flowing on their surfaces can locally heat the magnets changing their magnetic properties and, consequently, lowering their torque production capability and efficiency.

A common methodology to evaluate the eddy-current losses due to high order space harmonics is based on the comparison of analytical models and numerical FEM simulations [3]-[5]. Specific examples of determining surface losses in magnets forming a part of an electric motor, and their effective reduction through unconventional stator structures, known as "*modular*", can be found in [6], [7]. An alternative approach for estimating the surface losses is the search for empirical relationships based on coefficients determined by theoretical considerations or, more rarely, by measurements [8]-[10] or by combining measurement results and analytical relationships [11], [12]. From this viewpoint, the accurate measure of the surface losses can be still considered an open research field [13]. In particular, it is an authors' opinion that the construction of special prototypes and the definition of dedicated test procedures is the correct pathway to approach the problem rigorously.

The main purpose of this study is to present an original modelling approach based on FEM simulations that enables the determination of surface losses due to the presence of high order space harmonics in the air gap magnetic field distribution. Furthermore, the difference in the spatial distribution of losses on the rotor surface of electric machines resulting from the adopted model will be discussed with the final target to quantify the phenomenon and, consequently, to understand its 'measurability'.

II. THE MODELING CONCEPTS

The analytical models described in the literature usually adopt formulations and coefficients determined for the axial magnetization case (i.e. flux density waveform parallel to the lamination plane, stationary in the space and pulsating in the time). According to Turowski *et al.* [14], there is a significant difference between the losses determined for the axial magnetization (with a specific maximum amplitude of the flux density) and the losses resulting from a magnetization with the same flux density waveform, but rotating in circumferential direction over the ferromagnetic sheet (i.e. still parallel to its lamination plane). This is due to the different paths of the eddy currents induced in the sheet cross surface faced with the air gap for the two magnetization cases – see Fig. 1.

In the present work, the authors extend this fundamental finding by taking into account the physical fact that multiple current loops are present in the lamination sheet surface – see Fig. 1.b. Moreover, a reliable model should reflect as accurately as possible the physical phenomenon in the form of changes in magnetic flux in the air gap, for example, of an induction motor. In standard motor production, the stator windings are embedded in discrete slots and they create the step-like mmf waveform at the air gap. For the winding construction, semi-closed slot are necessarily used, introducing the well-known perturbations in the spatial distributions of the magnetic field present at the air gap.

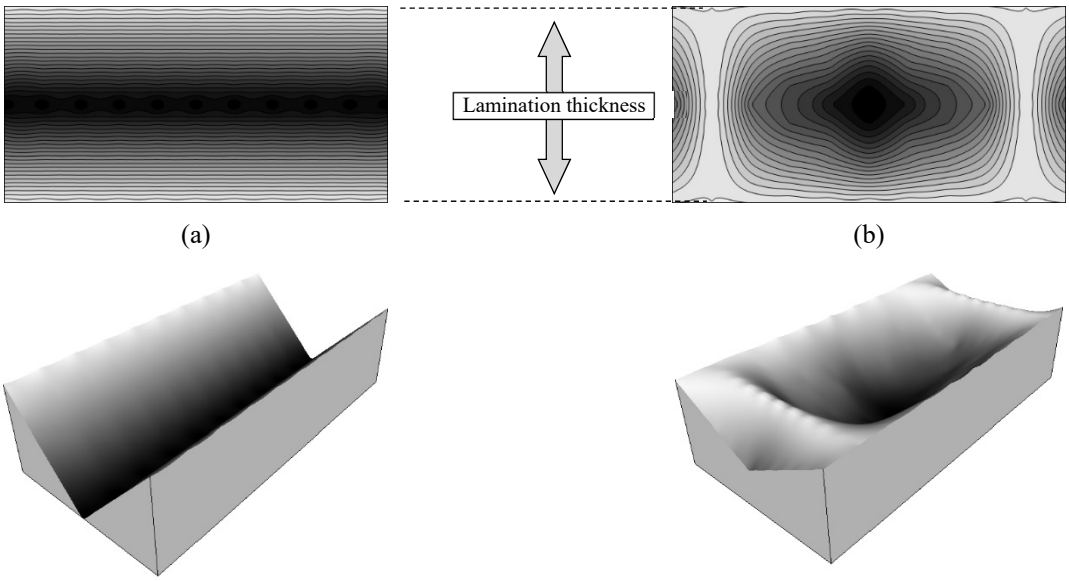

Fig.1. The instantaneous distributions of eddy currents and their envelopes (in gray) on the lamination surface faced with the air gap: a) induced by axial magnetization, b) induced by rotating magnetic field over the ferromagnetic surface.

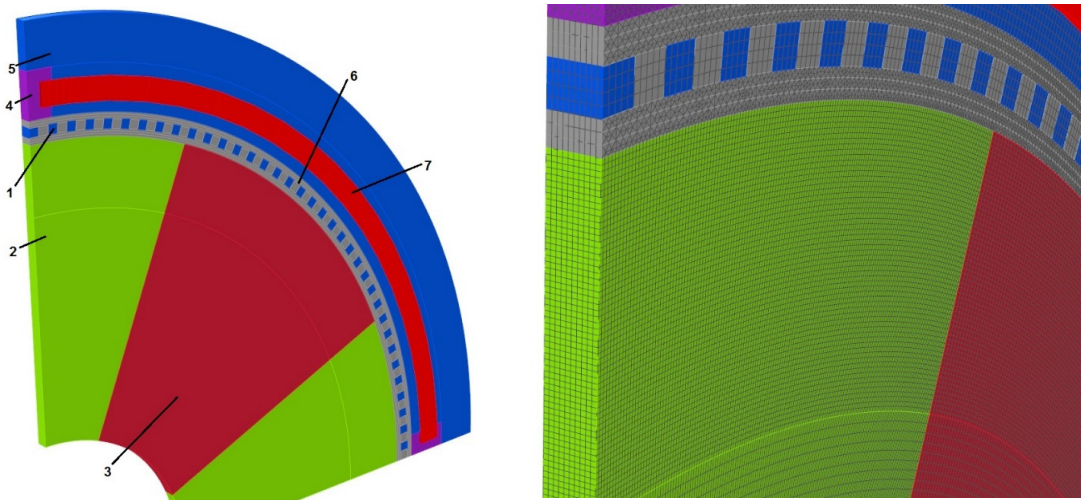

Fig.2. The simplified 3D-FEM model, the model mesh (on the right) and its area subdivision (1 – flux concentrators; 2 – rotor yoke; 3 – rotor yoke for loss measurements, 4 – stator slot, 5 – stator yoke, 6 – air gap, 7 – excitation coil).

Thus, along the rotor circumference there are regions in which there is relatively high flux densities and adjacent areas with significantly lower values. Therefore, moving high order harmonics are present in the spatial distribution of the air gap flux density waveform. During normal operations, the slip of these harmonics is close to one and eddy currents are induced in the rotor surface. These currents flow into each lamination in paths similar to those shown in Fig. 1.b, generating the so-called '*surface losses*'.

On the basis of the authors' experience, any attempt to compute the surface losses by means of a 3D-FEM model of the real motor geometry (i.e. rotor core made of insulated laminations and winding distribution) is doomed to failure. In fact, also neglecting the short circuits on the rotor surface between adjacent laminations (e.g. resulting from the technological process), the generated eddy currents flow within each lamination in many loops along the circumferential direction. To solve the problem, the authors propose a simplified 3D-FEM model constituted by a single lamination sheet and a single excitation coil, where the uneven spatial distribution of the flux density is 'synthetized' by using 'flux concentrators' (i.e. high permeability elements) suitably shaped and positioned in the air gap –see Fig. 2. This original artifice is essential to reflect the nature of the physical phenomena that occur in the real cases. In fact, from the physical phenomenon point of view, the relative movement between the flux density harmonics and the rotor surface can be emulated considering stationary both the air gap field distribution and the rotor, while only the flux concentrators rotates. This assumption enables the concept that just a single excitation dc coil is enough to model correctly the movement of the high order harmonics.

In the model shown in Fig. 2, particular attention has been paid to the definition of the equivalent air gap thickness, which should be the same or close to the value of the actual machine. For the case of study, the two layers adjacent to the stator and rotor surfaces have a thickness of 0.2 mm, while the layer for the positioning of the high permeability elements has a height equal to 0.3 mm.

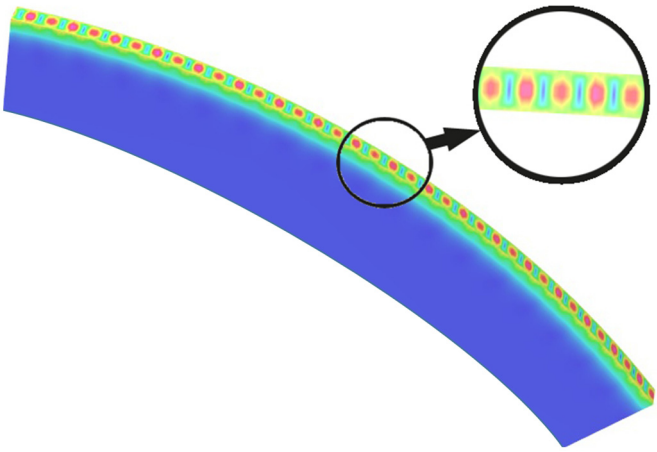

Fig.3. Eddy current distribution in the rotor region close to the air gap.

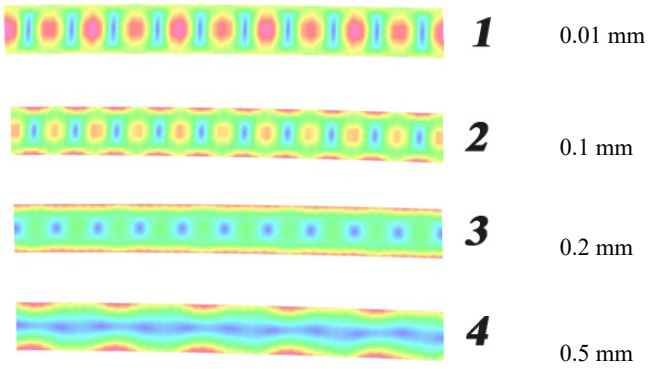

Fig.4. Eddy current distribution in rotor lamination cross sections at different radial distance from the air gap.

It is important to remark that region 3 shown in Fig. 2, was separated by the other parts of the rotor lamination to avoid any influence of the stator slot and excitation coil presence on the magnetic field distribution over the rotor and, consequently, on the surface losses. It should be mentioned that only the eddy current losses are analyzed in the proposed model, neglecting the hysteresis losses. In the calculations, a constant relative magnetic permeability was assumed (e.g. 1000 for the rotor and 10000 for both the flux concentrators and the stator) and the dc current in the stator coil was regulated to obtain the desired amplitude of air gap flux density harmonics.

The high permeability elements moving in the air gap have a defined geometrical width and rotational speed. The element width is used to define the harmonic content of the spatial flux density distribution, while the speed value sets the frequencies of the induced eddy currents. Note that by properly shaping the profile of the flux concentrators and their positioning, it is possible to create a quasi-sinusoidal flux density distribution. This modeling technique could be of potential interest when sinusoidal spatial distributions are not featured in the used FEM software.

Finally, it was observed that the accuracy of eddy current mapping induced in the rotor lamination depends on the quality of the mesh. Just as an example, the mesh density is shown on the right side of Fig. 2. The use of second-order elements for the grid allows for the precise determination of the magnetic field distribution for harmonics with frequencies up to 20 kHz, which is considered sufficient for the conducted analysis.

III. Selected 3D-FEM Results

The proposed 3D-FEM model has been initially tested adopting the same value for the distance between adjacent flux concentrators and their circumferential width (i.e. ratio width / distance = 1). In the simulations, the 36 flux concentrators (spread over 1/4 of the circumference) rotate in the speed range of 30-600 rpm and generate a moving flux density waveform having the specified flux density amplitude (resulting from the used DC excitation current). Examples of the induced current density distributions in the lamination cross surfaces near the air gap, determined for concentrators rotating at the 480 rpm, are shown in Fig. 3 and Fig. 4.

Figure 4 clearly shows that the induced current density distribution is similar to the typical distribution of the axial magnetization solution (see Fig. 1.a) only in the rotor lamination cross section at the distance of 0.5 mm from the surface facing the air gap. Vice versa, the current '*vortexes*' of the theoretical case reported in Fig. 1.b are clearly visible in the lamination cross section at the distance of 0.01 mm from the outer lamination surface.

The value of Joule losses can be determined performing the volumetric integral of the product of the electric field intensity and the eddy current density in the elements of region 3 shown in Fig. 2. Then, the surface loss density is determined as the ratio of the computed Joule losses over the surface of the considered sector faced to the airgap. For the case study, when the amplitude of the imposed harmonic (having frequency of 1152 Hz at the speed of 480 rpm) is 0.279 T, the surface loss density has been estimated equal to 4.3 W/m^2.

To prove the negligible influence of the relative magnetic permeability on the generated surface losses, the computations have been repeated changing the permeability of the rotor yoke for loss measurements (i.e. region 3 in Fig. 2) in the FEM model. In particular, relative permeability of 500, 1000 and 2000 have been assumed. Also for these analyses, the ratio width / distance between concentrators has been considered equal to 1. The concentrators rotated at 240 rpm, and the radial component B_R of the fundamental flux density harmonic in the air gap was 280 mT at the frequency of 576 Hz. The following results have been obtained:

- for $\mu_r = 500 \rightarrow$ surface loss density = 1.02 W/m^2;
- for $\mu_r = 1000 \rightarrow$ surface loss density = 1.03 W/m^2;
- for $\mu_r = 2000 \rightarrow$ surface loss density = 1.04 W/m^2.

After the initial calculations were completed, the task was to determine the surface losses generated by harmonics of a specific frequency and amplitude. Because the concentrators can rotate at a given speed, it is possible to generate a fundamental harmonic of a given frequency. The change of excitation current allows adjusting the amplitude of this harmonic. However, the FEM analyses prove that, when the ratio concentrators width / distance = 1, it can be assumed that the distribution of the induction radial component B_R (in the air gap between the concentrators and the surface of the rotor part where the surface losses are estimated) is quasi-sinusoidal, with an error in determining the surface losses lower than 2%. The calculation results for few selected harmonics with given frequencies and amplitudes are listed in Table I.

TABLE I
FEM CALCULATION RESULTS: SURFACE LOSSES GENERATED BY SELECTED HARMONICS FOR THE RATIO 1:1

Harmonic amplitude, (mT)	Surface iron losses, (W/m^2)					
	144 Hz	288 Hz	576 Hz	864 Hz	1152 Hz	1440 Hz
50	0.006	0.008	0.036	0.074	0.129	0.200
100	0.024	0.034	0.144	0.296	0.516	0.798
150	0.054	0.076	0.324	0.665	1.163	1.796
200	0.096	0.135	0.577	1.182	2.066	3.194
250	0.150	0.211	0.901	1.848	3.228	4.990
300	0.216	0.303	1.298	2.660	4.648	7.186

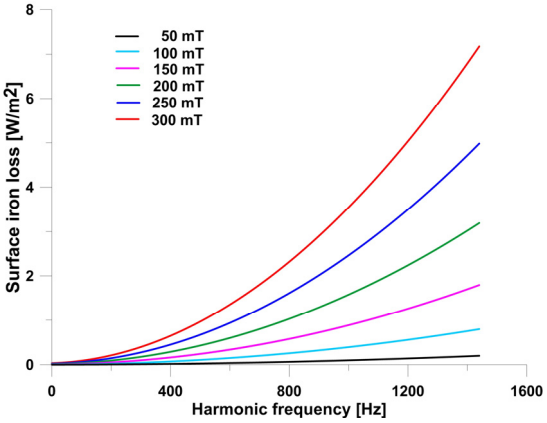

Fig.5. Surface iron loss vs. harmonic frequency.

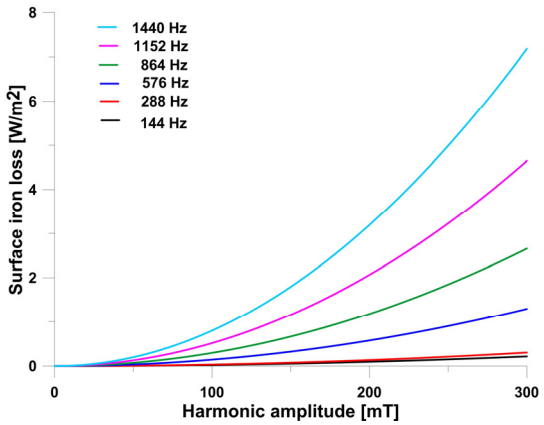

Fig.6. Surface iron loss vs. harmonic amplitude.

Based on the calculations for selected harmonics having specified frequency and amplitude, approximations of surface losses versus frequency and versus harmonic amplitude were obtained and plotted in Fig. 5 and Fig. 6.

The next step of the research work was to build a model where the relation between concentrators width and their distance would correspond to a situation from a real motor with a specific number of stator slots. In detail, a model in which the ratio is equal to 4:1 and the flux concentrators rotate at 480 rpm has been analyzed. This corresponds to a situation where the stator slot opening width is 1/5 of the stator slot pitch. The distribution of the induced eddy currents for such a case is shown in Fig. 7, whereas the waveform of the flux density radial component B_R at the air gap between concentrators and the rotor surface is presented in Fig. 8. The Fourier series of the above waveform is reported in Table II.

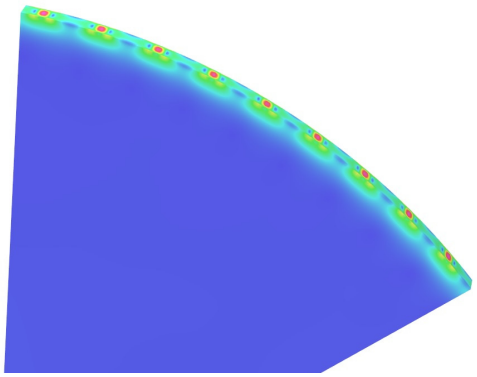
Fig.7. Eddy current distribution in rotor lamination for the FEM model with ratio 4:1.

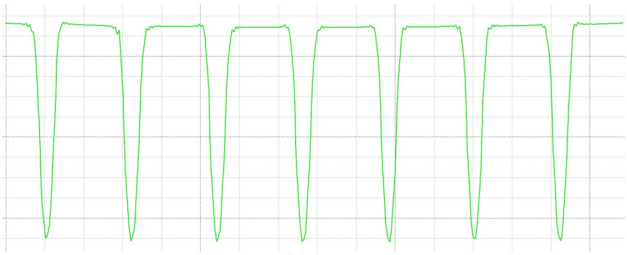
Fig.8. Calculated waveform of flux density radial component B_R, at middle of air gap, for the FEM model with ratio 4:1, over 1/4 of circumference.

TABLE II
HARMONICS OF THE FLUX DENSITY RADIAL COMPONENT AND RELATED SURFACE LOSS COMPONENTS FOR THE RATIO 4:1.

Harmonic frequency, (Hz) / harmonic order	Harmonic amplitude, (mT)	Surface loss generated by the harmonic, (W/m^2)
448 / 56	176	0.273
512 / 64	51	0.029
896 / 112	136	0.591
960 / 120	92	0.308
1024 / 128	30	0.037
1344 / 168	86	0.516
1408 / 176	120	1.099
1792 / 224	40	0.195
1856 / 232	41	0.207
2240 / 280	9	0.015
2688 / 336	6	0.010
3136 / 392	8	0.023
3584 / 448	3.6	0.007
4480 / 560	2	0.004
4928 / 616	1.9	0.004
5376 / 672	1	0.002

TABLE III
THE VALUES OF λ_ν COEFFICIENT USED FOR SURFACE LOSS CALCULATIONS, ACCORDING TO (2)

Harmonic order	56	64	112	120	128	168	176	224
λ_ν * 1e^{-4} (m)	5.6	4.9	2.8	2.6	2.45	1.85	1.80	1.14
Harmonic order	232	280	336	392	448	560	616	672
λ_ν * 1e^{-4} (m)	1.13	1.10	0.95	0.80	0.70	0.55	0.05	0.04

For the considered case of study, the surface losses calculated using the FEM model were 5.55 W/m^2, whereas the surface losses obtained by summing up the surface loss originating from individual harmonics (see Table II) resulted 3.32 W/m^2. During the summation, all significant harmonics of the waveform presented in Fig. 8 were taken into account. Comparing the surface losses computed by the FEM model with those obtained summing up the surface loss contribution of each individual harmonics, it was found that the second approach results only in 60% of the losses directly calculated by the FEM model.

IV. DISCUSSION

In literature, it is possible to find advanced analytical relationships allowing estimation of the surface losses, caused by the existence of the magnetic field spatial harmonics in the air gap. One of the more advanced descriptions can be found in [11]. The authors of this work propose the following analytical relationships.

$$P_{surf} = \sum_{\nu} p_\nu\left(B_\nu, f\nu\right)\rho S \lambda_\nu \qquad (1)$$

$$\lambda_\nu = \pi D /\left(2 p \nu\right) \qquad (2)$$

In (1) P_{surf} is the total surface loss caused by all spatial harmonics, ν is the harmonic order, $p_\nu(B_\nu, f_\nu)$ is the specific iron loss (determined under axial magnetization) for the ν-th harmonic, at B_ν flux density and f_ν frequency. Additionally, ρ is the material mass density, S is the surface area affected by spatial harmonics (including slot pitch and slot opening, rotor diameter as well as packing core factor) and λ_ν is the depth of field penetration for ν-th harmonic. In (2) p is the pole pair number, and D is the diameter of the surface area affected by spatial harmonics.

For the sake of completeness, it is important to mention the data used in the calculation:

- ρ = 7.62e^3 kg/m^3;
- D = 40e^{-3} m;
- $S = (2\pi \cdot 20e^{-3}) \cdot 0.5e^{-3}/8 = 7.85e^{-6}$ m^2 because the FEM model measuring region takes 1/8 of the circumference;
- 2p=4 poles.

Taking into account that the frequency of 448 Hz corresponds to the 56 harmonic order, the values of the λ_ν coefficient were computed and listed in Table III.

TABLE IV
SURFACE LOSS COMPONENTS, CALCULATED ACCORDING TO (1), FOR FEM MODEL HAVING RATIO 4:1.

Harmonic frequency (Hz)	Harmonic amplitude (mT)	Iron loss for axial magnetization (W/m^3)	Surface losses generated by harmonic (1) (W/m^2)
448	176	4523	2.53
512	51	652	0.31
896	136	11116	3.11
960	92	6222	1.63
1024	30	1218	0.30
1344	86	10811	2.01
1408	120	21741	3.87
1792	40	5512	0.76
1856	41	6130	0.82
2240	9	2168	0.24
2688	6	2681	0.25
3136	8	3970	0.31
3584	3.6	4136	0.28
4480	2	5748	0.32
4928	1.9	6750	0.34
5376	1	7475	0.35

The surface loss components and total surface loss are presented in Table IV. The total surface losses calculated by (1) are 17.45 W/m^2, approximately 3 times more than the losses calculated by the FEM model.

Reference [15] presents a simplified approach to determine surface losses, based on the use of the skin effect factor. In this approach, the author proposes (3) to quantify the phenomenon.

$$P_{surf} = \sum_{\nu} \left(P_{h\nu} + k_{sk} P_{ev} + P_{exv}\right) \qquad (3)$$

In (3) $P_{\mathrm{h}\nu}$, $P_{ex\nu}$ and $P_{\mathrm{e}\nu}$ are the hysteresis, the excess and the classical eddy current losses for ν-th harmonic, respectively. The coefficient k_{sk} is the skin effect factor given by the (4).

$$k_{sk} = \frac{3}{\lambda}\frac{\sinh(\lambda) - \sin(\lambda)}{\cosh(\lambda) - \cos(\lambda)} \qquad (4)$$

$$\lambda = \frac{d}{\delta} \qquad \delta = \frac{1}{\sqrt{\pi \nu \mu \gamma}}$$

In the previous equations, d is the lamination thickness, ν is the harmonic frequency, μ is the magnetic permeability and γ is the material electrical conductivity.

In [16] it is suggested to compute the surface losses using the modified penetration depth $\delta^* = \delta / 16$. In this way, the damping of the flux pulsations in the rotor laminations is equivalently taken into account. Additionally, from a practical point of view, to determine the surface losses originating from the spatial harmonics, the hysteresis losses can be ignored, and the excess losses can be combined with the losses due to eddy currents.

TABLE V
SURFACE LOSS COMPONENTS, CALCULATED ACCORDING TO (7), FOR FEM MODEL HAVING RATIO 4:1.

Harmonic frequency (Hz)	Harmonic amplitude (mT)	Specific iron loss for axial magnetization (W/m^3)	Penetration depth $\delta^* * 1e^{-5}$ (m)	λ parameter	k_{sk} parameter	Surface losses generated by harmonic (7) (W/m^2)
448	176	4523	3.33	0.938	0.999	2.53
512	51	652	3.11	1.001	0.999	0.32
896	136	11116	2.35	1.326	0.995	3.09
960	92	6222	2.27	1.373	0.994	1.62
1024	30	1218	2.20	1.416	0.993	0.29
1344	86	10811	1.92	1.623	0.989	1.99
1408	120	21741	1.87	1.666	0.988	3.82
1792	40	5512	1.66	1.880	0.980	0.75
1856	41	6130	1.63	1.908	0.979	0.81
2240	9	2168	1.48	2.100	0.970	0.23
2688	6	2681	1.36	2.293	0.959	0.23
3136	8	3970	1.25	2.487	0.944	0.30
3584	3.6	4136	1.18	2.646	0.910	0.26
4480	2	5748	1.05	2.976	0.896	0.26
4928	1.9	6750	1.00	3.125	0.878	0.3
5376	1	7475	0.96	3.246	0.862	0.3

In order to compare the results with those obtained from FEM model, the following analytical formula was used where δ is the penetration depth, σ is material mass density, p_{ev} is the specific eddy current loss for ν-th harmonic and axial magnetization.

$$P_{surf} = \sum_{v} \left(k_{sk}\, p_{ev}\, \delta^*\, \sigma \right) \qquad (7)$$

The results of these calculations are presented in Table V. By applying (7) the calculated total surface losses are 17.15 W/m^2, once again almost 3 times more than the losses calculated by the FEM model.

V. CONCLUSION

With this study the authors point out the possibility to estimate the surface loss per m^2, without the need to calculate penetration depth and to use the eddy current losses measured for axial magnetization. The obtained results were compared with those obtained by other analytical models already available in literature, in order to provide a complete scenario for the quantification of this challenging phenomenon. It has been verified that the surface losses calculated according to the considered analytical equations based on axial magnetization loss data are about three times those calculated by the FEM model. Additionally, in presence of distorted flux density waveforms at the air gap (e.g. as in the case of a ratio width/distance = 4:1 for the concentrators), the surface losses calculated by adding the losses originating from individual harmonics are lower than 40% with respect to the losses computed by the used professional FEM software (able to account for the deformed waveforms). Therefore, being direct measurements very difficult or even impossible, further researches with different distortion levels of the air gap flux density waveforms will be undertaken to explain the aforementioned differences in the values of surface losses calculated by the proposed approaches.

REFERENCES

[1] E. Fornasiero, N. Bianchi, and S. Bolognani, "Slot harmonic impact on rotor losses in fractional-slot permanent-magnet machines", *IEEE Trans. Ind. Electron.*, vol.59, pp.2557-2564, 2012.

[2] A. Cavagnino, S. Vaschetto, L. Ferraris, Z. Gmyrek, E. B. Agamloh, and G. Bramerdorfer, "Striving for the highest efficiency class with minimal impact for induction motor manufacturers", *IEEE Trans. Ind. Appl.*, vol.56, pp.194-204, 2020.

[3] K. Atallah, D. Howe, P.H. Meller, and D.A. Stone, "Rotor loss in permanent-magnet brushless AC machines", *IEEE Trans. Ind. Appl.*, vol. 36, no. 6, pp.1612-1618, 2000.

[4] H. Toda, Z. Xia, J. Wang, K. Atallah, and D. Howe, "Rotor eddy-current loss in permanent magnet brushless machines", *IEEE Trans. Magnetics*, vol. 40, no. 4, pp. 2104-2106, 2004.

[5] S.-H. Han, T. M. Jahns, and Z. Q. Zhu, "Analysis of rotor core eddy-current losses in interior permanent magnet synchronous machines", Proc. of 2008 IEEE Industry Applications Society Annual Meeting, pp.1-8, 2008.

[6] K. Atallah, and D. Howe, "Modular permanent magnet brushless machines for aerospace and automotive applications", Proc. 20thInt. Workshop Rare-Earth Magnets and Their Applications, 2000, pp. 1039–1048.

[7] T. Oikawa, T.Tajima, K. Matsumoto, H. Akita, H. Kawaguchi, and H. Kometani, "Development of high efficiency brushless DC motor with new manufacturing method of stator for compressors", Proc. 16th Int. Compressor Engineering Conf., CD12-4, 2002.

[8] K. Komeza, and M. Dems, "Finite-element and analytical calculations of no-load core losses in energy-saving induction motors", *IEEE Trans. Ind. Electron.*, vol.59, pp.2934-2946, 2012.

[9] N. Bianchi, S. Bolognani, and E, Fornasiero, "An overview of rotor losses determination in three-phase fractional-slot PM machines", *IEEE Trans. Ind. Appl.*, vol.46, pp.2338-2345, 2010.

[10] N. Bianchi, and E. Fornasiero, "Index of rotor losses in three-phase fractional-slot permanent magnet machines", *IET Electr. Power Appl.*, vol. 3, pp. 381–388, 2009.

[11] M. Dems, and K. Komeza, "The influence of electrical sheet on the core losses at no-load and full-load of small power induction motors", *IEEE Trans. Ind. Electron.*, vol. 64, no 3, pp.2433-2442, 2017.

[12] H. B. Ertan, K. Leblebicioglu, B. Avenoglu, and M. Pirgaip, "High-frequency loss calculation in a smooth rotor induction motor using FEM", *IEEE Trans. Energy Conversions*, vol.22, no 3, pp.566-575, 2007.

[13] H. Kofler, "Stray load losses in induction machines. A review of experimental measuring methods and a critical performance evaluation", *Renewable Energy & Power Quality Journal*, vol.1, pp.318-323, 2003.

[14] J. Turowski, and M. Turowski, "Engineerings electrodynamics. Electric machines, transformer, and power equipment design", *CRC Press*, 2014.

[15] B. A. Nasir, "An accurate iron core loss model in equivalent circuit of induction machine", *Hindawi Journal of Energy*, article ID 7613737, 2020.

[16] M. M. Kostic, "Calculation improvement of no-load stray losses in induction motors with experimental validation", *Serbian Journal of Electrical Engineering*, vol.12, no 3, pp.303-320 , 2015.